THE JOURNAL OF COMPARATIVE NEUROLOGY 483:476–488 (2005)

Cellular and Network Properties of the Subiculum in the Pilocarpine Model of Temporal Lobe Epilepsy

ANDREAS KNOPP,[1] ANATOL KIVI,[1] CHRISTIAN WOZNY,[1] UWE HEINEMANN,[2] JOACHIM BEHR[1]*

[1]Neuroscience Research Center of the Charité, Humboldt University of Berlin, D-10117 Berlin, Germany

[2]Johannes-Müller-Institute of Physiology, Charité, Humboldt University of Berlin, D-10117 Berlin, Germany

ABSTRACT

The subiculum was recently shown to be crucially involved in the generation of interictal activity in human temporal lobe epilepsy. Using the pilocarpine model of epilepsy, this study examines the anatomical substrates for network hyperexcitability recorded in the subiculum. Regular- and burst-spiking subicular pyramidal cells were stained with fluorescence dyes and reconstructed to analyze seizure-induced alterations of the dendritic and axonal system. In control animals burst-spiking cells outnumbered regular-spiking cells by about two to one. Regular- and burst-spiking cells were characterized by extensive axonal branching and autapse-like contacts, suggesting a high intrinsic connectivity. In addition, subicular axons projecting to CA1 indicate a CA1-subiculum-CA1 circuit. In the subiculum of pilocarpine-treated rats we found an enhanced network excitability characterized by spontaneous rhythmic activity, polysynaptic responses, and all-or-none evoked bursts of action potentials. In pilocarpine-treated rats the subiculum showed cell loss of about 30%. The ratio of regular- and burst-spiking cells was practically inverse as compared to control preparations. A reduced arborization and spine density in the proximal part of the apical dendrites suggests a partial deafferentiation from CA1. In pilocarpine-treated rats no increased axonal outgrowth of pyramidal cells was observed. Hence, axonal sprouting of subicular pyramidal cells is not mandatory for the development of the pathological events. We suggest that pilocarpine-induced seizures cause an unmasking or strengthening of synaptic contacts within the recurrent subicular network. J. Comp. Neurol. 483:476–488, 2005.

Indexing terms: hippocampus; subiculum; CA1; dendrites; axons; morphology

Hippocampal sclerosis is a neuropathological hallmark of many patients with temporal lobe epilepsy (TLE). It is characterized by a pronounced cell loss and gliosis in the dentate hilus, the CA3 and CA1 region of the hippocampus, while the adjacent subiculum remains largely intact (Mathern et al., 1997; Fisher et al., 1998). Given that in patients with severe hippocampal sclerosis CA3 and CA1 are involved in seizure generation, it is feasible that in the course of TLE the subiculum undergoes an epileptogenic plasticity that results in a secondary seizure focus. This hypothesis is supported by a recent study in hippocampal brain slices of patients with TLE and hippocampal sclerosis showing spontaneous, epileptiform activity in the subiculum and never in CA3 or CA1 (Cohen et al., 2002, 2003). The spontaneous activity remained in the isolated subiculum, suggesting an autonomous epileptic focus in this brain region. We found that even in nonsclerotic hippocampal tissue, subicular pyramidal cells show spontaneous epileptiform rhythmic activity (Wozny et al., 2003). In both studies this spontaneous activity closely resembled the discharges seen in EEG records of the TLE pa-

Grant sponsor: Deutsche Forschungsgemeinschaft; Grant number: SFB-TR 3.

*Correspondence to: Joachim Behr, Neuroscience Research Center of the Charité, Humboldt University of Berlin, Schumannstrasse 20/21, D-10117 Berlin, Germany. E-mail: joachim.behr@charite.de

Received 27 January 2004; Revised 16 August 2004; Accepted 3 November 2004

DOI 10.1002/cne.20460

Published online in Wiley InterScience (www.interscience.wiley.com).

tients, supporting the contribution of the subiculum in ictogenesis. These observations suggest an ongoing epileptogenic plasticity in the subiculum as a consequence of the persistent epileptic input from CA1.

Recurrent excitatory connectivity of neurons and a high density of pacemaker cells are critical factors for the generation of synchronized activity (Heinemann, 1987), conditions the subiculum complies with: The rat subiculum is characterized by the abundance of bursting neurons, which fire clusters of action potentials at high frequency (O'Mara et al., 2001) and by an intrinsic connectivity that may serve to synchronize synaptic activity (Behr and Heinemann, 1996; Harris and Stewart, 2001; Harris et al., 2001). In spite of these cellular and network properties that construct a seizure-prone structure, the mechanisms that finally induce synchronized activity were hitherto not understood.

Hippocampal sclerosis is associated with network plasticity that comprises dendritic alterations and axonal sprouting. Previous studies have consistently reported reductions in dendritic spine density and a loss of dendritic branches of pyramidal cells in human (Scheibel et al., 1974; Isokawa and Levesque, 1991) and experimental TLE (Nadler et al., 1980; Phelps et al., 1991; Drakew et al., 1996). These morphological alterations of the dendritic system have important consequences for neuronal information processing. Several studies in different experimental models of TLE indicate that the enhanced neuronal excitability of CA1 pyramidal cells after partial deafferentiation from CA3 is caused by a reinnervation of CA1 pyramidal cells that originates from recurrent axon collaterals occupying vacated synaptic sites (Perez, 1996; Esclapez, 1999; Smith and Dudek, 2001). Likewise, deafferentiation of the subicular pyramidal cells due to cell loss in CA1 and the subsequent formation of excitatory recurrent connections between subicular principal cells may cause an enhanced excitability. In addition, subicular pyramidal cells may sprout to the vacated synaptic sites in CA1 as recently proposed (Lehmann et al., 2001). An understanding of the local connectivity of subicular neurons and their interaction with CA1 pyramidal cells are therefore critical for understanding the subiculum as a seizure focus.

Using the pilocarpine model of epilepsy, this study examines morphological alterations of subicular pyramidal cells as a cause for network hyperexcitability in the subiculum. Pilocarpine administration causes a convulsive status epilepticus (SE) that leads to neuronal injury that mimics human hippocampal sclerosis and develops spontaneous seizures after a latent period of several weeks following SE. Hypotension, hyperpyrexia, hypoglycemia, acidosis, and hypoxia, all of which are associated with SE, may also contribute to seizure generation after pilocarpine treatment (Turski et al., 1989; Walker et al., 2002). Regular-spiking and burst-spiking subicular pyramidal cells were stained with fluorescent dyes and reconstructed to analyze seizure-induced alterations of the dendritic and axonal system. We show that, in contrast to CA1, neither an increase of burst-spiking cells nor axonal sprouting to vacated synaptic sites account for the enhanced network excitability observed in the subiculum of pilocarpine-treated rats.

MATERIALS AND METHODS

Pilocarpine model of epilepsy

The experiments were conducted in accordance with the guidelines of the European Communities Council and were approved by the Regional Berlin Animal Ethics Committee (G 0269/95, G 0328/98). Wistar rats 4–5 weeks old (150–230 g) were injected with the muscarinic agonist pilocarpine (350 mg/kg i.p.). Peripheral cholinergic effects were reduced by pretreatment with methylscopolamine (1 mg/kg s.c.) 30 minutes before pilocarpine administration. Then, 10–30 minutes after pilocarpine injection the animals developed a generalized convulsive SE. In order to terminate SE, diazepam (5–10 mg/kg i.p.) was injected 80 minutes after onset. Subsequently, the behavioral signs of the SE disappeared about 1 hour later. The animals were kept thereafter in separate cages on a standard light/dark cycle. The animals went through a seizure-free interval of about 2 weeks. After 6–8 weeks the rats (400–600 g) were observed by videorecording for 3–10 days. Only animals showing spontaneous seizures were selected for experiments. These animals developed 1.8 ± 0.4 seizures per 24 hours ($n = 52$ rats). Age-matched animals were used as controls.

Preparation of slices

The rats were decapitated under deep ether anesthesia. The brains were quickly removed and washed with cooled (4°C) aerated (95% O_2, 5% CO_2) artificial cerebrospinal fluid (ACSF) containing, in mM: NaCl 129, NaH_2PO_4 1.25, $NaHCO_3$ 21, KCl 3, $CaCl_2$ 1.6, $MgSO_4$ 1.8, glucose 10, pH 7.4. Horizontal slices of 400 μm containing the entorhinal cortex, the subiculum, and the hippocampus were prepared with a Campden vibroslicer (Loughborough, UK). The slices were transferred into an interface chamber continuously perfused with aerated, prewarmed (34°C) ACSF.

Staining with fluorescence dyes

Before staining with fluorescein (fluoro-emerald) or tetramethylrhodamine (rhodamine, fluoro-ruby; Molecular Probes, Leiden, The Netherlands) a period of 2 hours without further manipulation was strictly observed to permit sealing of damaged fibers, as described previously (Glover et al., 1986; Boulton et al., 1992; Lehmann et al., 2001). A small dye-crumb was taken up by the sharp tip of a glass pipette. Then the pipette tip was introduced vertically into the stratum radiatum of the CA1 region in order to injure a number of neurons by which the dye was taken up. Resealing and distribution of the dye within the neurons was allowed for 3–6 hours. Stained slices were used for patch-clamp recordings (after ≥3 hours) or were fixed (after about 6 hours) overnight in 4% paraformaldehyde dissolved in 0.1 M sodium phosphate buffer (PB, pH 7.4). After impregnation with 30% sucrose in 0.1 M PB, serial sections (thickness 50 μm) of the slices were prepared by using a freezing microtome (Leitz; Leica Microsystems, Wetzlar, Germany). The sections were mounted on gelatin-coated slides, air-dried, placed under a coverslip by use of a nonfluorescent mounting medium (Citifluor AF1; Agar, Germany), and stored in darkness at 6°C.

Biocytin staining

In patch-clamp experiments, one neuron per slice was loaded with biocytin in order to investigate its morphol-

ogy. For this purpose, 0.5% biocytin was added to the electrode solution. Dye loading of the cell was allowed for 30–45 minutes. After withdrawing the pipette, distribution of the dye within the neuron was allowed for additional 30–60 minutes. Then the slice was fixed overnight as described above and incubated for 24 hours in PB supplemented with 1% Triton X-100 and 0.001% avidin-biotin-horseradish peroxidase complex. After washing with PB the slices were dehydrated with ethanol, mounted on slides, and covered with Citifluor AF1 (Agar).

Nissl stain

For Nissl staining, hippocampal sections (50 μm) were mounted on slides, dehydrated in graded ethanol/xylene, rehydrated, and incubated in 0.5% aqueous cresyl violet for 1.5–2 minutes. After decolorizing the sections in a solution of 100 μl acetic acid and 200 ml ethanol (50%), they were again dehydrated and then coverslipped with Depex (Serva, Heidelberg, Germany). Nissl-stained pyramidal neurons were counted in an area of $235 \times 390\ \mu m^2$ in the middle segment of the subiculum, where the electrophysiological recordings were conducted.

Electrophysiology

Electrophysiological recordings from subicular neurons were conducted during perfusion with ACSF at 32 ± 2°C. In experiments where $GABA_A$ receptors were blocked, ACSF was supplemented with bicuculline methiodide (5 μM) and $CaCl_2$ and $MgSO_4$ concentrations were increased to 4 mM. Recordings were performed in the middle portion of the subiculum with respect to the CA1-subiculum axis in order to avoid recordings of neurons at the boundary from CA1 to the subiculum. Microelectrodes were prepared from borosilicate glass tubings. All single-cell recordings were performed by patch-clamp technique except the experiments on synaptic properties of subicular pyramidal cells, which were conducted with sharp microelectrodes.

Extra- and intracellular measurements. Recordings were performed in a liquid–gas interface chamber. Extracellular microelectrodes were filled with ACSF and had a resistance of 1–3 M°. Sharp microelectrodes for intracellular recordings were filled with 2.5 M K^+-acetate and had a resistance of 50–100 MΩ. An amplifier SEC10L (npi Instruments, Tamm, Germany) was used in conventional bridge mode. Signals were filtered at 3 kHz, sampled, and collected using a TIDA interface (HEKA, Lambrecht/Pfalz, Germany). Field potentials and single-cell EPSPs were evoked using 100-μs pulses every 10 seconds with glass-insulated bipolar platinum wire electrodes (tip separation 50–100 μm).

Patch-clamp recordings. Patch-clamp recordings were performed in a submerged recording chamber in current-clamp whole-cell mode. Microelectrodes of 1.5–5 MΩ were filled with K^+-gluconate 135, KCl 6, $MgCl_2$ 2, HEPES 10, pH 7.3 (KOH). Visualization of single neurons was established by an Olympus BX51WI microscope equipped with infrared illumination. Fluorescein- and tetramethylrhodamine-labeled neurons were visualized by excitation with an Hg lamp (Olympus U-RFL-T) at a wavelength of 510–550 nm and 470–490 nm, respectively, and observed at >570 and 510–550 nm, respectively (filters U-MWG2 and U-MNIBA2). Cells chosen for recordings had a pronounced main apical dendrite perpendicular to the alveus and at least two basal dendrites. The typical shape of pyramidal neurons was confirmed in all reconstructed biocytin-filled cells. Data were collected with an RK-100 patch-clamp amplifier at 10 kHz bandwidth. Recordings and analysis were done using ISO2 software (MFK, Niedernhausen, Germany). All traces were recorded with a sampling rate of 10 kHz (12-bit resolution).

In general, only cells with resting membrane potentials more negative than –50 mV and overshooting action potentials were accepted. To characterize the cells' discharge behavior, depolarizing current steps of 800 or 1200 ms duration (0.1-1.0 nA) were applied at resting membrane potential (RMP) and at hyperpolarized holding potentials. The input resistance R_{in} of a cell was determined at RMP at steady state responses to current pulses of –0.1 nA.

Statistics

Statistical evaluation was performed by applying Student's *t*-test (Excel, Microsoft, Redmond, WA) or by Fisher's test; data are expressed as means ± SEM. The significance level was set at $P < 0.05$.

Microscopy and image preparation

Biocytin-labeled neurons were visualized by an upright confocal microscope (Leica, Heidelberg, Germany) equipped with a 10× or 20× water-immersion objective (NA 0.5, Leica). For visualization of dendritic spines and axons we used a 20× water-immersion objective with high aperture (NA 0.95, Olympus). Excitation was established by use of an argon/krypton laser at a wavelength of 488 nm. Stacks of optical sections (1024 × 1024 pixels in the xy plane) were acquired by separation of 1–3 μm in the z-axis. Images taken by confocal microscopy were analyzed off-line using NIH software Image J (v. 1.29, W. Rasband). Fluorescent somata in the subiculum after application of fluorescent tracers were evaluated using a microscope (Leica) fitted with fluorescence equipment. At an excitation wavelength of 480 nm (filter set L5) fluorescein fluorescence was visualized as intense green and at an excitation wavelength of 546 nm (filter set G/R) rhodamine fluorescence was visualized as intense red emission. Nissl-stained neurons were counted by use of a microscope (Zeiss Axioscope, Zeiss, Oberkochen, Germany) and KIB 2.6 software (KAPPA opto-electronics, Gleichen, Germany). Images were stored in Tif-format and assembled by CorelDraw 11.0 (Corel, Unterschleissheim, Germany).

RESULTS

Cellular and synaptic properties

In accordance with previous reports (Staff et al., 2000; Jung et al., 2001; Menendez de la Prida et al., 2003), a broad variation of firing behavior of subicular pyramidal cells was observed. In both control and pilocarpine-treated rats neurons showed regular-, burst-, strong burst-, and high threshold burst-spiking behavior in response to depolarizing current pulses (Fig. 1A). Regular-spiking cells showed trains of single action potentials during depolarizing current injections. In burst-spiking cells, depolarization above threshold caused an initial burst of 2–3 action potentials. Strong burst-spiking neurons responded with more than one burst of action potentials in the course of the depolarizing current injection. High threshold burst-spiking cells responded with single action potentials at threshold depolarization, but displayed bursts of action

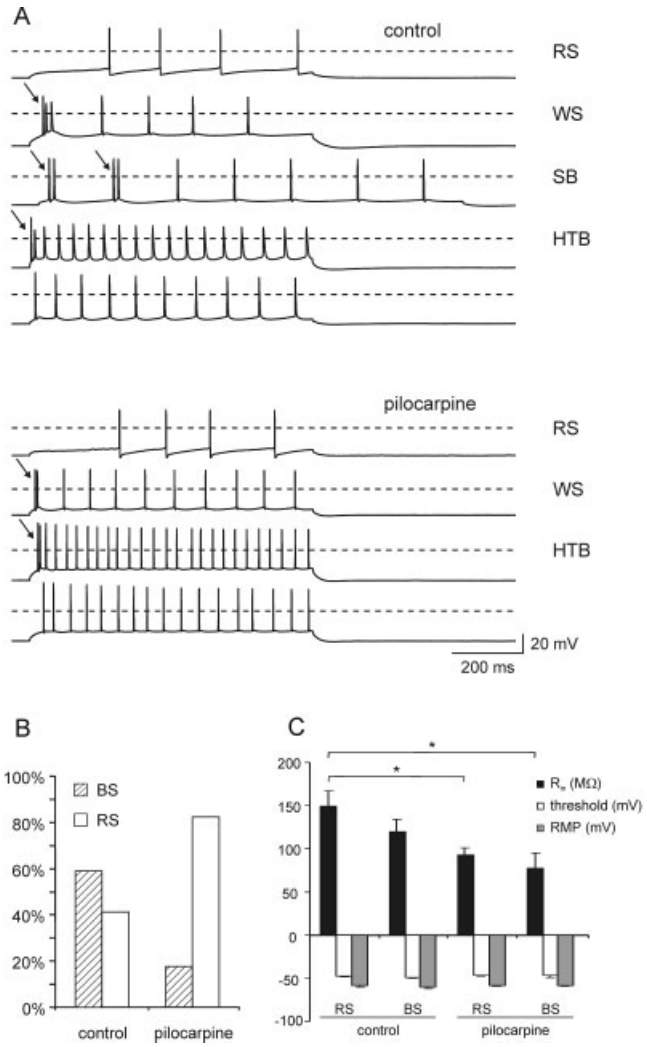

Fig. 1. Membrane properties of subicular pyramidal cells in control and pilocarpine-treated rats determined by whole-cell patch-clamp recordings. **A:** Discharge behavior of subicular pyramidal cells: In both animal groups neurons were classified as regular-spiking (RS), weak burst-spiking (WB), strong burst-spiking (SB), and high threshold burst-spiking cells (HTB), depending on their spiking behavior in response to depolarizing current pulses (see text). Bursts of spikes are indicated by arrows. **B:** Fraction of regular- and burst-spiking pyramidal cells (WB, SB, and HTB were pooled). Note the decreased fraction of burst-spiking cells in pilocarpine-treated rats. **C:** Input resistance (R_{in}), threshold, and resting membrane potential (RMP) of regular- and burst-spiking subicular pyramidal cells. In pilocarpine-treated animals the input resistance was different from controls.

potentials when the depolarizing current injection was increased. For further analysis we pooled all types of burst-spiking cells. Hence, the major division of subicular pyramidal cells was into burst- and regular-spiking cells.

In accordance with previous studies (O'Mara et al., 2001) in control rats, the majority (59%, n = 27) of neurons was classified as burst-spiking cells (Fig. 1B). In pilocarpine-treated rats the fraction of burst-spiking cells was significantly reduced (18%, n = 17), as shown by Fisher's test ($P < 0.001$). Resting membrane potential and spike threshold were similar in regular-spiking and burst-spiking cells of each animal group and no significant difference was found between control and pilocarpine-treated rats. Pyramidal cells from pilocarpine-treated rats, however, showed a reduced input-resistance, especially if compared to regular-spiking control cells (Fig. 1C).

Frequently, but not consistently, we observed spontaneous rhythmic activity at a frequency of 0.5–2 Hz, as illustrated in simultaneous intra- and extracellular recordings (Fig. 2A). This activity was never seen in control slices. As previously described (Behr et al., 1998), stimulation of CA1 efferents caused regular EPSPs in subicular pyramidal cells of control animals (n = 10, Fig. 2C). Increasing the stimulation intensity caused action potential firing. In pilocarpine-treated rats, however, one-third of the cells responded with an EPSP that was followed by a second one (n = 3 out of 9 cells, recorded from eight rats). Upon increasing stimulation intensity the second EPSP, but not the first, gave rise to a burst of action potentials (Fig. $2D_1$). In cells where a second EPSP was absent, this could be evoked after application of the $GABA_A$ receptor-antagonist bicuculline in pilocarpine-treated rats (n = 5, Fig. $2D_2$) but never in controls (n = 10, Fig. 2C). Upon stronger stimulation, a small EPSP suddenly resulted in abnormal all-or-none bursts of action potentials in pilocarpine-treated rats but not in controls. The second EPSP had typical features of a polysynaptic network-driven event (Miles and Wong, 1987a; Crepel et al., 1997): its latency decreased with increasing stimulation intensity (Fig. 2E,F).

Morphological network properties

To estimate the subicular cell loss we determined the density of neurons in Nissl-stained sections (56 sections from eight control and 39 sections from five pilocarpine-treated rats). Cells were collected in a rectangular area within the subiculum subdivided into five columns parallel to the CA1-subiculum axis (Fig. 3). The neuronal density was 40,470 ± 980 cells/mm^3 in control rats. In pilocarpine-treated rats the density was significantly reduced by 35% as compared to control rats (26,250 ± 930 cells/mm^3, Fig. 3). The neuronal density in both control and pilocarpine-treated rats was distributed uniformly along the CA1-subiculum axis.

Subicular pyramidal cells of control (n = 15) and pilocarpine-treated rats (n = 14) were filled with biocytin by the patch-clamp electrode. Part of the selected cells (control: n = 6; pilocarpine: n = 4) were superficial neurons with the soma located at the border between the pyramidal and the molecular layer. All cells were reconstructed to analyze seizure-induced alterations of the dendritic and axonal system. Electrophysiological characterization revealed the same fraction of regular- and burst-spiking cells as for the unlabeled cells: in control animals 7 out of 13 neurons and in pilocarpine-treated rats 3 out of 10 neurons were burst-spiking cells. In pyramidal cells of both animal groups numerous basal dendrites arborized within the pyramidal layer (Fig. 4A). The primary apical dendrite branched extensively within the molecular layer, with thin branches reaching down to the fissure. In principle, branching of the primary apical dendrite occurred not before entering the molecular layer. Only about half of the cells with the soma situated deep in the pyramidal layer showed a primary apical dendrite, with very thin and short dendritic branches perpendicular to the main

apical dendrite before it left the pyramidal layer. The arborization of the apical dendrites was quantified by determining the order number of the branching points (Perez et al., 1996). Plotting the mean number of branching points for each order number revealed that branching points with order numbers between 6 and 8 were reduced in epileptic rats (Fig. 4B). This result suggests a reduced dendritic arborization of the proximal apical dendrites in pilocarpine-treated rats, as illustrated by the enlargements in Figure 4A. Length and width of the apical and basal dendritic tree of the reconstructed neurons from control and pilocarpine-treated rats were similar (Fig. 5A). The apical dendritic tree ran along the alvear-fissural axis or was tilted either to CA1 or to the presubiculum. For a quantitative analysis of the tilt from each cell, the balance point location of the apical dendritic tree was determined with respect to a coordinate system. The soma represented the origin, the abscissa paralleled the alveus, and the ordinate represented the alvear-fissural axis (see Fig. 5B). For a single neuron the spacing (x-value) between its balance point and the alvear-fissural axis was taken as a measure of the tilt of the apical dendritic tree. The mean value of all balance points was not different between control (x = 9.9 ± 57 μm, y = 344 ± 24 μm; n = 15) and pilocarpine-treated rats (x = –23 ± 57 μm, y = 352 ± 32 μm; n = 14). Nine neurons (30%) showed a tilt of more than x = 50 μm. These most extremely tilted cells were found in both control (n = 4 out of 15) and pilocarpine-treated rats (n = 5 out of 14; no significant difference). They were located in the superficial (n = 4 out of 10) and in the deep region (n = 5 out of 19; no significant difference) of the pyramidal layer.

Subicular pyramidal cells of both animal groups exhibited spiny dendrites (Fig. 6A). The spine density was dependent on the region and on the diameter of the dendrites. Primary dendrites (>2 μm) were almost free of spines. Distal apical dendrites (<0.5 μm) also showed a remarkable low spine density. We selected dendrites with a diameter of ~1 μm to evaluate the spine density (Fig. 6B). In control rats the spine density was almost the same for basal and distal apical dendrites (7.8 ± 1.1 and 6.0 ± 0.9 spines per 10 μm, respectively, n = 10). Proximal dendrites of control rats, however, showed a spine density that was 2-fold higher than that of basal and distal dendrites (13.0 ± 1.0 spines per 10 μm, n = 10). This result reflects a high density of synaptic contacts in the proximal apical dendritic compartment of the subiculum, which is known to be strongly innervated by CA1 axons (Amaral et al., 1991). The spine density determined for basal and distal dendrites of pilocarpine-treated rats was not significantly different from control rats (7.6 ± 1.1 and 5.8 ± 0.9 spines per 10 μm, respectively, n = 10). Proximal dendrites in pilocarpine-treated rats, however, displayed a significantly lower density of spines than in controls

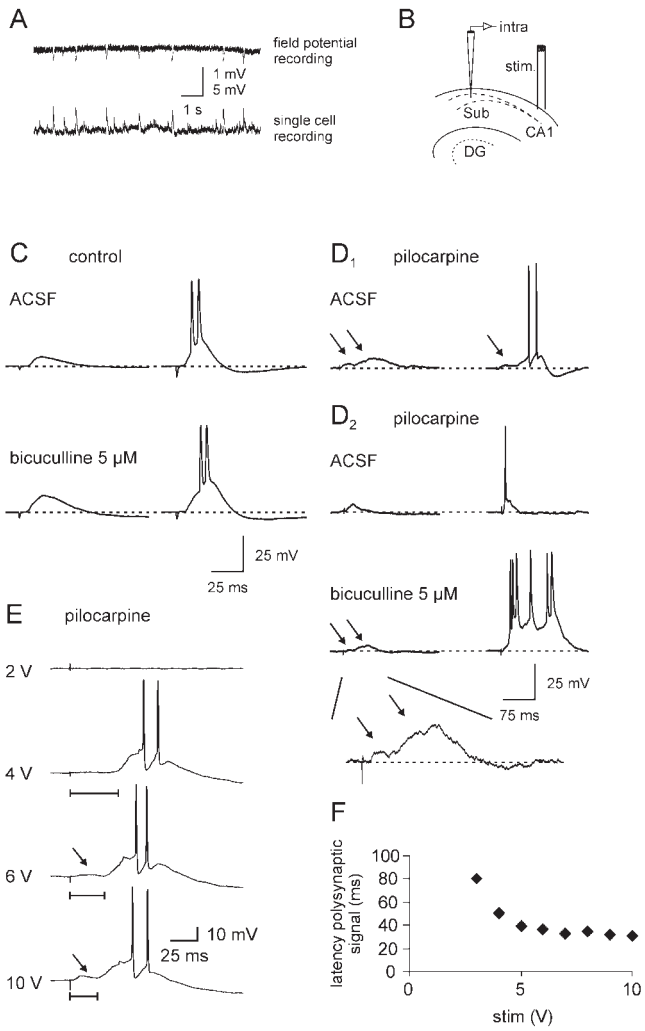

Fig. 2. Synaptic properties of subicular pyramidal cells in control and pilocarpine-treated rats. **A:** Simultaneous records of field potential and single cell recordings revealed spontaneous synchronized activity in the subiculum of pilocarpine-treated rats. Note the different voltage scales: field potential recording, 1 mV; single cell recording, 5 mV. **B:** Experimental configuration: Placement of the recording electrode in the subiculum. Stimulation electrode was placed in the alveus. Sub, subiculum; DG, dentate gyrus; CA1, area CA1. Intracellular recordings after stimulation of the alvear pathway. **C:** EPSP in control slices (upper left trace). Increasing stimulation intensity caused action potential firing (upper right trace). In the presence of the $GABA_A$ receptor-antagonist bicuculline (5 μM) the EPSP amplitude increased (lower left trace), but the pattern of action potential firing was nearly unaltered (lower right trace). **D_1:** In pilocarpine-treated animals, frequently a second EPSP component was elicited (left trace). The first and second EPSP are marked by arrows. Upon increasing the stimulation intensity the second EPSP generated a burst of action potentials (right trace). **D_2:** In those cells which did not show a second EPSP (upper traces), this could be elicited by application of the $GABA_A$ receptor-antagonist bicuculline in pilocarpine-treated rats (lower left trace). For clarity, the two EPSPs are also shown with a 6-fold magnification in amplitude and stretched in time by factor 3 (lower trace). Increased stimulation intensity caused a long-lasting burst of action potentials revealing hyperexcitability in subicular neurons of pilocarpine-treated rats (lower right trace). Please note the different time scales for traces obtained from control and pilocarpine-treated animals. **E:** In the presence of the $GABA_A$ receptor antagonist bicuculline a long-latency burst of action potentials was generated. Increasing stimulus intensity shortened the latency of the second EPSP indicating a polysynaptic event (see bars below traces). Stimuli above 6 V generated a preceding second EPSP with a latency comparable to those recorded in control cells (see arrow). **F:** Plotting the latency of the second EPSP upon the stimulation intensity shows the typical dependency of polysynaptic-driven network responses.

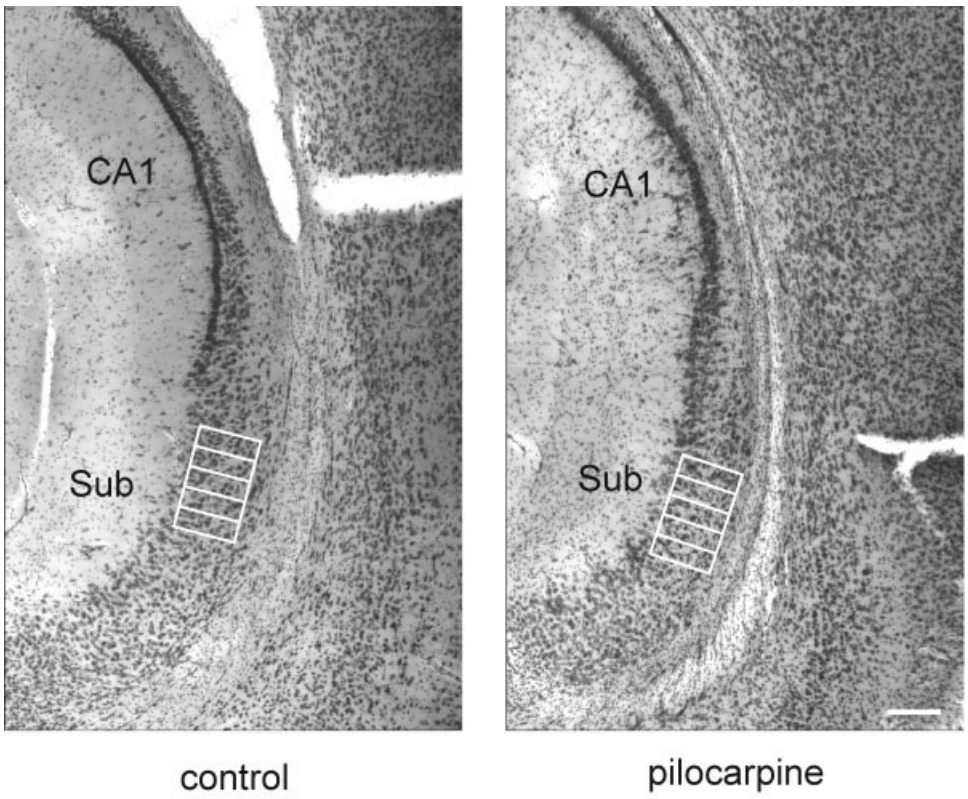

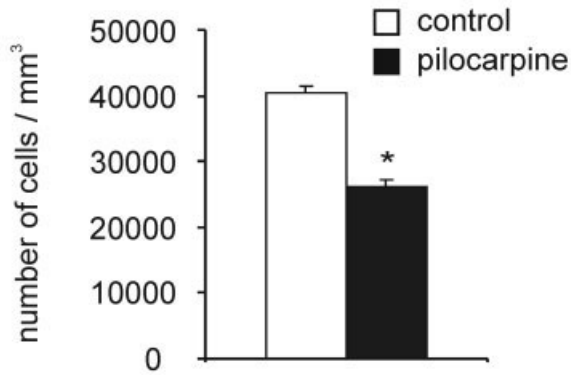

Fig. 3. Density of pyramidal neurons in the subiculum of control and pilocarpine-treated rats. Nissl-stained slice from a control and a pilocarpine-treated rat showing CA1 and the subiculum. Rectangular areas were used for counting stained neurons in the subiculum. In pilocarpine-treated rats the neuronal density was significantly lower than in control rats. Sub, subiculum. Scale bar = 200 μm.

(8.4 ± 0.8 spines per 10 μm, n = 9). As the spine loss reduces the membrane surface it might be associated with an increase of the input resistance R_{in}. However, we observed a reduction of R_{in} after spine loss (Fig 6C).

Axons could be distinguished from dendrites by the lack of spines and a uniform diameter over long distances. The main axon left the soma at its basal site or, as observed in one cell, at the proximal part of a basal dendrite. Reconstructed axons of subicular pyramidal cells of control (n = 7 cells) and pilocarpine-treated animals (n = 5 cells) branched extensively throughout the stratum pyramidale and moleculare (Fig. 7A,B). The quantification of the axonal collateralization by Scholl analysis revealed no difference between control and pilocarpine-treated rats (Fig. 7C). Labeled axons were fine and lined with multiple varicosities (Fig. $7D_3$). Only axons leaving the subiculum via the alveus never showed varicosities (Fig. 7E). In one control and three pilocarpine-treated animals, axon collaterals were observed in close proximity to the soma (not shown) or close (<1 μm) to spiny basal dendrites of the same cell (Fig. 7D,E). Figure $7D_1$ shows a varicosity of the axon shown in Figure D_3 being situated between two dendritic spines of the basal dendrite shown in Figure D_2.

As recently described (Berger et al., 1980; Köhler, 1985; Lehmann et al., 2001; Commins et al., 2001; Harris and Steward, 2001a,b; Harris et al., 2001), few subicular pyramidal cells of control and pilocarpine-treated rats showed axon collaterals that headed to CA1 and termi-

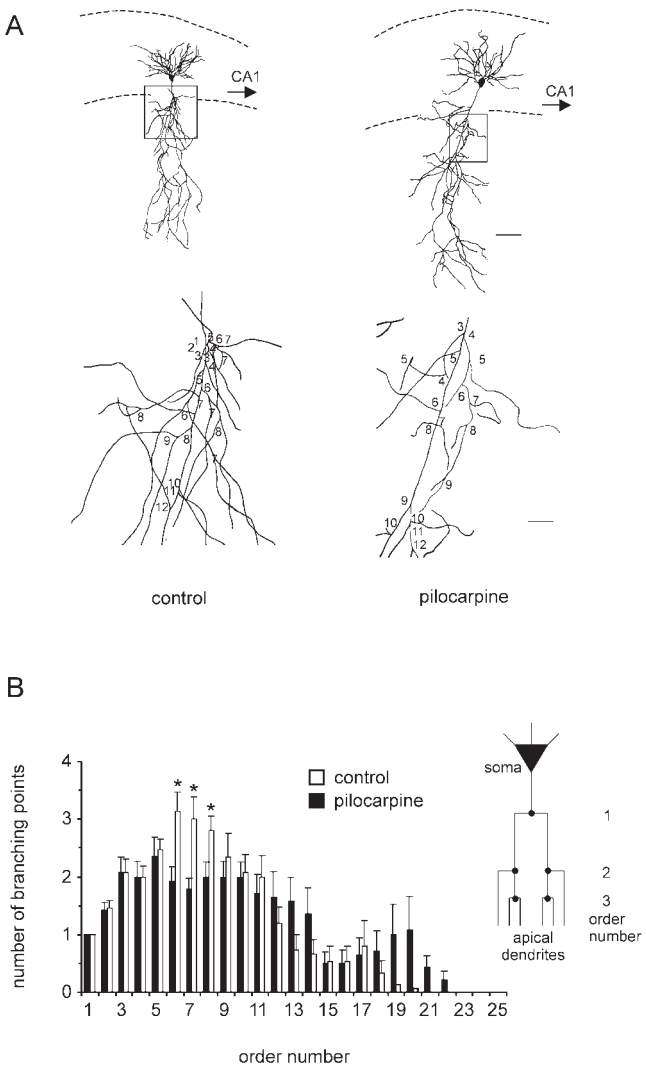

Fig. 4. Dendritic system of subicular pyramidal cells in control and pilocarpine-treated rats. **A:** Reconstructions of biocytin-filled pyramidal cells from a control and a pilocarpine-treated rat. The dashed lines represent the borders of stratum pyramidale. Arrows indicate the orientation of the cells in the slice. The proximal part of apical dendrites enclosed by the rectangle is shown below at an enlarged scale. Dendritic branching points are indicated by their order number. **B:** Arborization of apical dendrites. The mean number of branching points per neuron is plotted on the order number of each branching point. Branching points were evaluated as shown in the scheme. Note the decreased number of branching points in the pilocarpine rat between the sixth and eighth order number. Scale bars = 100 μm in A (top); 20 μm in A (bottom).

nated in stratum radiatum and stratum pyramidale, respectively. We hypothesized that an enhanced projection of subicular pyramidal cells back to vacated synaptic sites in CA1 in pilocarpine-treated rats might reinforce sustained epileptiform activity between CA1 and the subiculum. To quantify the number of subicular pyramidal cells projecting to CA1 we enabled these cells to take up a fluorescent tracer by injury of their axons in stratum radiatum of CA1 and extracellular application of fluorescein or tetramethylrhodamine. This method caused staining of cell somata in the subiculum by retrograde axonal transport of the fluorescent dye. In control rats (4 animals, 50 sections) 1.86 ± 0.37 labeled neurons were found per 50 μm section (Fig. $8A_1$). In pilocarpine-treated rats (10 animals, 238 sections) the number of fluorescent cells was not significantly different (2.14 ± 0.19 cells per section). The fraction of sections with the same number of retrograde stained neurons also revealed no difference between control and pilocarpine-treated rats (Fig. $8A_2$). These results indicate that in control and pilocarpine-treated rats a comparable number of cells shows axon collaterals projecting to stratum radiatum of CA1. In order to determine whether this projection is cell-type-specific, we performed patch-clamp recordings of retrograde labeled subicular pyramidal cells. In pilocarpine-treated rats (n = 14) 29% of these neurons were classified as burst-spiking cells (Fig. 8B,C). The remaining cells were regular-spiking cells. This ratio of burst-spiking and regular-spiking cells corresponds to the one shown in Figure 1B, suggesting that we have no evidence for a cell-specific projection to CA1.

DISCUSSION

The present study demonstrates that the subiculum of pilocarpine-treated rats shows an enhanced network excitability. It is characterized by spontaneous rhythmic activity, polysynaptic responses, and all-or-none evoked bursts of action potentials. To examine anatomical substrates for the hyperexcitability within the subicular network, pyramidal cells were electrophysiologically classified and their dendritic and axonal system was reconstructed. In control preparations burst-spiking cells outnumbered regular-spiking cell by about two to one. Both cell types were characterized by an extensive axonal branching within the subiculum and back to CA1 as well as by autapses-like contacts, suggesting a high intrinsic connectivity under control conditions. In pilocarpine-treated rats the subiculum showed cell loss of about 30%, which was paralleled by a dramatic decrease in the number of sampled burst-spiking cells. Arborization and spine density in the proximal part of the apical dendrites were significantly decreased in pilocarpine-treated rats, suggesting a partial deafferentiation from CA1. Subicular pyramidal cells of pilocarpine-treated rats did not show an aberrant axonal sprouting. Hence, sprouting is no prerequisite for the development of pathological events in the subiculum. We suggest that pilocarpine-induced seizures cause an unmasking or strengthening of synaptic contacts within the recurrent subicular network.

Synaptic and cellular properties

An important feature of the rat subiculum is the high fraction (50–100%) of burst-spiking neurons which fire clusters of action potentials at high frequency (Mason, 1993; Mattia, 1993; Taube, 1993; Behr et al., 1996; Staff et al., 2000; Jung et al., 2001; Menendez de la Prida et al., 2003). An abundance of burst-spiking cells is believed to predispose brain regions to generate synchronized activity (Jensen and Yaari, 1997; Yaari and Beck, 2002). Interestingly, in pilocarpine-treated rats the ratio of regular- to burst-spiking cells was practically inverse compared to the ratio observed in control preparations. This result agrees with the observation that intrinsic firing properties may be persistently affected by SE (Yaari and Beck, 2002). In control rats subicular burst-spiking depends on a Ca^{2+}

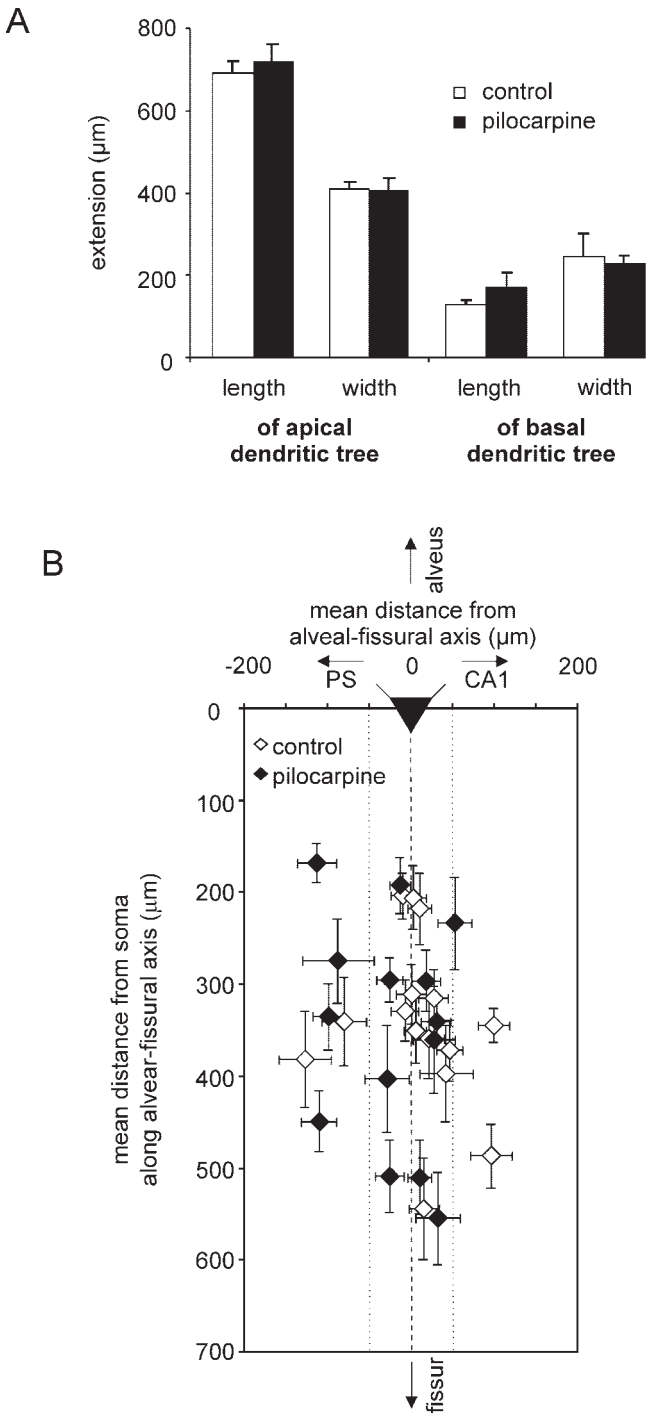

Fig. 5. **A:** Length and width of the apical (left) and basal (right) dendritic tree were not different between control and pilocarpine-treated rats. **B:** Balance points of apical dendritic trees. The soma of each reconstructed neuron was located at the (0;0) point of the coordinate system. Abscissa parallels the alveus and ordinate represents the alvear-fissural axis (indicated by dashed line). The coordinates of apical dendritic endpoints were determined and averaged for each neuron. Thus, each value represents the averaged location of all apical dendritic endpoints of one neuron (balance point of apical dendritic tree). Data points between the dotted lines were defined as minimal or no tilt (x-value of balance point between –50 and +50 µm). Four out of 15 neurons from control and 5 out of 14 neurons from pilocarpine-treated rats showed a remarkable tilt (x-value of balance point beyond –50 or +50 µm).

conductance which is not observed in regular-spiking neurons (Jung et al., 2001; Wellmer et al., 2002). Hence, the changed ratio of cell types in the subiculum of pilocarpine-treated rats might be caused by a loss of burst-spiking cells as a consequence of an enhanced bursting-associated excitotoxic Ca^{2+} influx during SE. Indeed, in pilocarpine-treated rats the total number of neurons was correspondingly decreased. Likewise, the cell-specific loss of layer III neurons of the entorhinal cortex in various in vivo models of epilepsy (Du et al., 1995) seems to rely on a cell-type-dependent increase in Ca^{2+} concentration during seizures (Gloveli et al., 1999). The ratio of regular-spiking and burst-spiking cells observed in pilocarpine-treated rats is comparable to the one shown in the subiculum of human epileptic tissue (Wozny et al., 2003). However, our data are in sharp contrast to a previous study that reported an increased fraction of burst-spiking cells in pilocarpine-treated rats (Wellmer et al., 2002). This discrepancy is most likely due to a difference in the recording site. While our recordings were preferentially conducted in the middle portion of the subiculum, Wellmer et al. recorded in the proximal part of the subiculum adjacent to CA1 (Wellmer, Beck, and Yaari, pers. commun.). This may explain that in control preparations the authors classified only 39% of the recorded cells as burst-spiking cells. This fraction of burst-spiking cells is far below the one recorded by us and others (see Introduction). In control and epileptic rats the pyramidal cells of the proximal subiculum seem to express membrane properties reminiscent of CA1 pyramidal cells. SE seems to convert regular-spiking cells in CA1 into intrinsic burst-spiking cells by selectively increasing the T-type Ca^{2+} current (Sanabria et al., 2001; Su et al., 2002). Hence, membrane properties and their seizure-induced alterations seem to be differentially expressed and regulated dependent on the region within the subiculum.

In pilocarpine-treated rats the subiculum displayed synchronous spontaneous rhythmic activity, similar to that described in the subiculum of patients suffering from pharmacoresistent TLE (Cohen et al., 2002; Wozny et al., 2003). In pilocarpine-treated rats subthreshold stimulation generated polysynaptic network-driven responses that gave rise to all-or-none bursts of action potentials. In cells where we did not observe recurrent excitatory responses, these could be triggered by application of the $GABA_A$ receptor antagonist bicuculline. This result indicates that in the subiculum of pilocarpine-treated animals $GABA_A$ receptor-mediated synaptic inhibition is of particular importance for controlling glutamatergic neurotransmission. Once eliminated, the strong potential of the recurrent excitatory network to produce epileptiform discharges is unleashed. This observation is in line with a recent study by Menendez de la Prida (2003) that suggests an inhibitory control of burst-spiking by local interneurons. Even though depolarizing GABAergic responses were shown to be involved in spontaneous rhythmic activity in human epileptic tissue (Cohen et al., 2002), in pilocarpine-treated rats the predominant network effect of GABAergic transmission seems to be inhibitory.

Dendritic system

The subiculum receives strong input from CA1 (Finch and Babb, 1981; Tamamaki and Nojyo, 1990; Amaral et al., 1991) and layer III of the entorhinal cortex (Steward and Scoville, 1976; Witter and Amaral, 1991; Witter, 1993) and relays

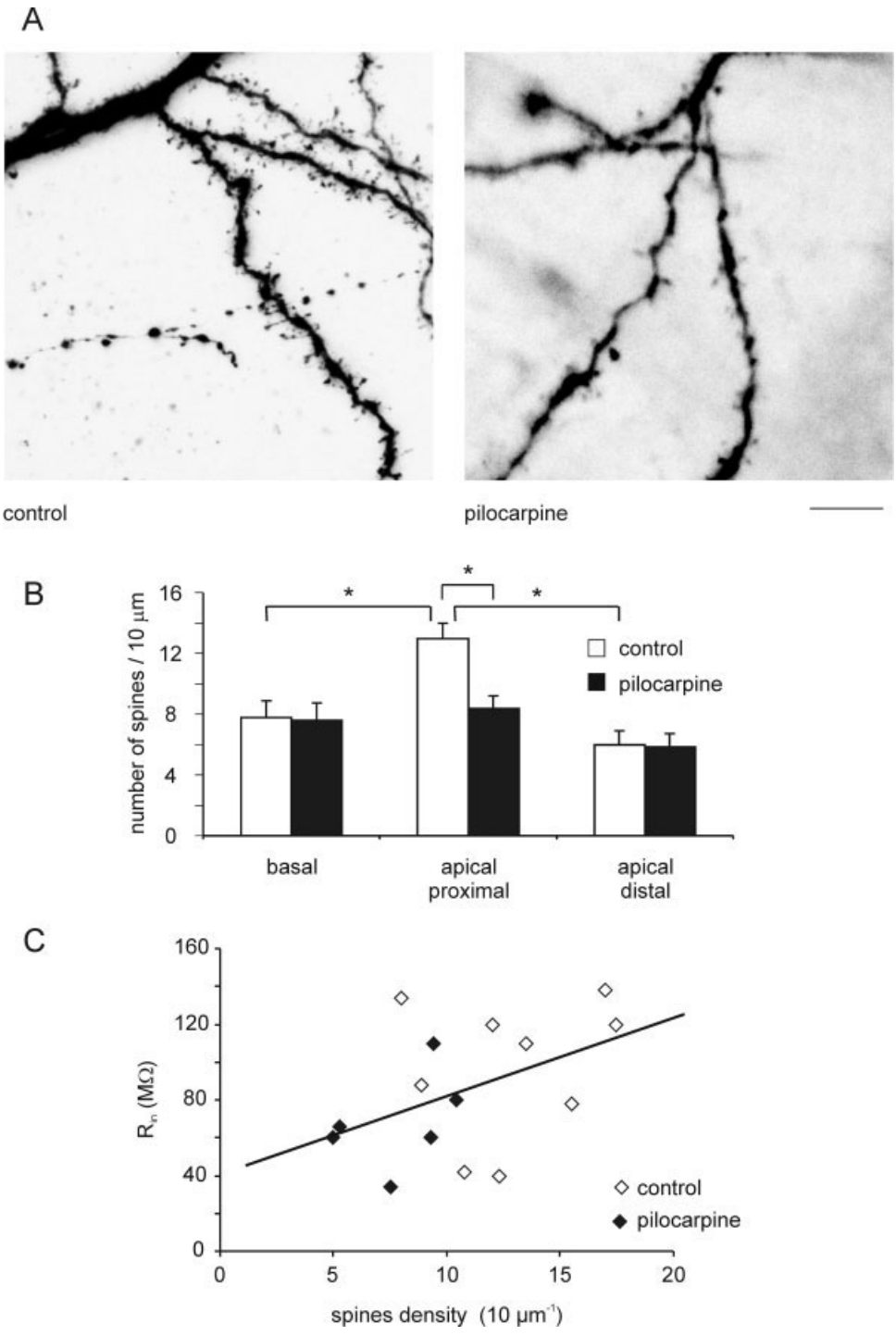

Fig. 6. Spine density of basal and apical dendrites in the subiculum. **A:** Biocytin-labeled dendrites from a control and a pilocarpine-treated rat. Images were obtained in the region of the proximal apical dendrites. Note the reduced spine density in pilocarpine-treated rats as compared to controls. **B:** Number of spines determined over a length of 10 µm from dendrites with a diameter of ~1 µm. In control rats the spine density of proximal dendrites was about 2-fold higher than that of basal and distal dendrites. Proximal dendrites of pilocarpine-treated rats displayed a significantly lower spine density than of control rats. **C:** Correlation of spine density and input resistance. Linear regression (solid line; slope = 4.1136, R^2 = 0.2051) was performed by use of all data points obtained from control and pilocarpine-treated rats. Scale bar = 10 µm in A.

information to other regions of the subicular complex, to the deep and superficial layers of the entorhinal cortex, as well as to a variety of distant cortical and subcortical structures as medial prefrontal cortex, retrosplenial cortex, nucleus accumbens, thalamus, and amygdala (Witter and Groenewegen, 1990; Witter et al., 1990; Witter, 1993; Greene, 1996). Entorhinal and hippocampal efferents terminate at different portions of the dendritic arbor of subicular pyramidal cells. While CA1 efferents terminate at basal dendrites and at the proximal part of the apical dendritic tree (Amaral et al.; 1991), entorhinal efferents synapse terminate preferentially at the distal compartment of the apical dendrites (van Groen et al., 2003). Most of the biocytin-stained cells were electrophysiologically classified. In agreement with previous studies (Finch et al., 1983; Mason 1993; Mattia et al., 1997; Staff et al., 2000; Harris et al., 2001), in control slices (n = 13 cells)

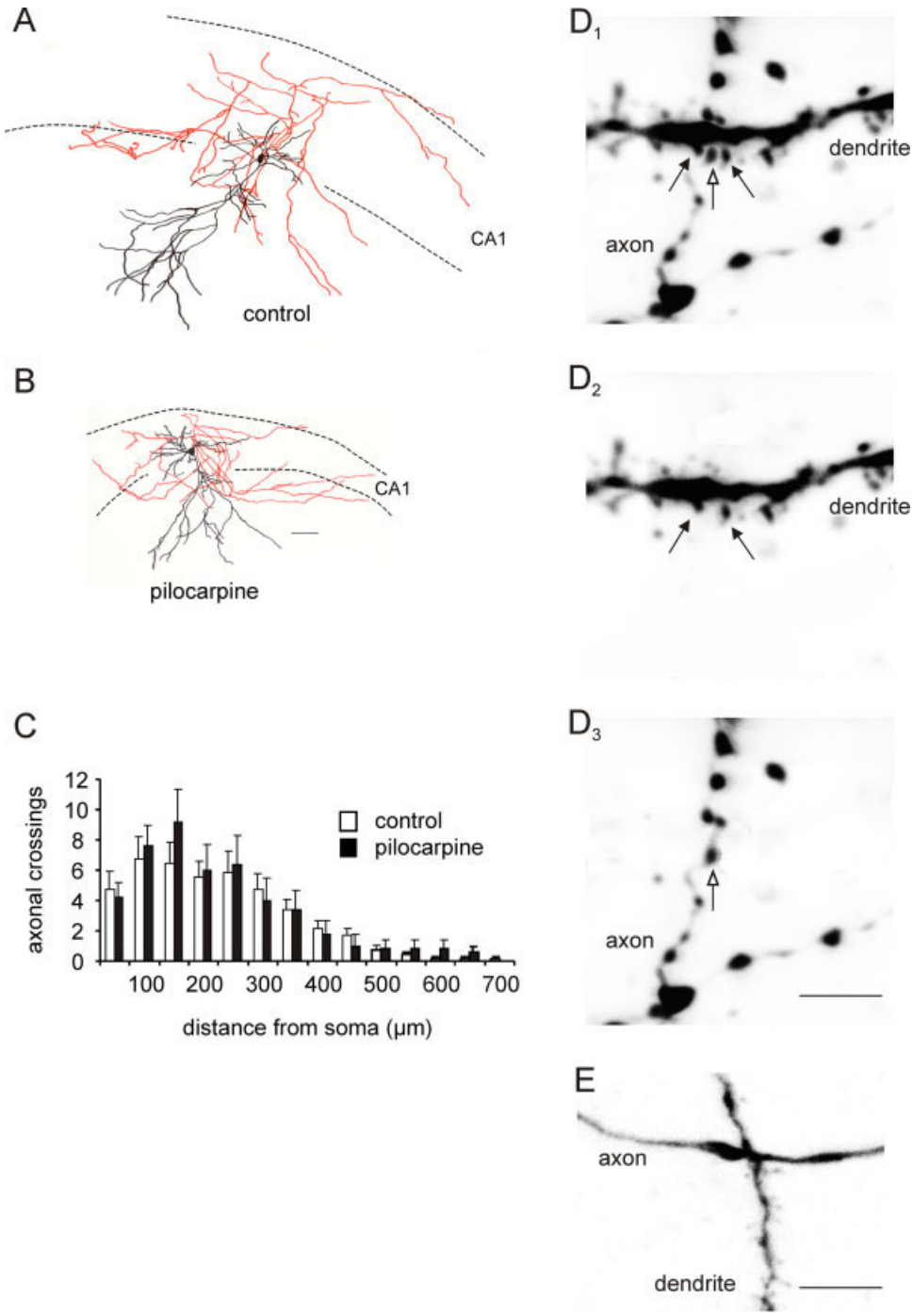

Fig. 7. Axonal collateralization. **A,B:** Two pyramidal cells from a control and a pilocarpine-treated rat showing extensive axonal branching. Axons spread widely throughout the stratum pyramidale and stratum moleculare. Axon collaterals project to stratum pyramidale and stratum radiatum of CA1. **C:** Scholl analysis of axonal collateralization showing numbers of axonal crossings with the concentric Scholl rings drawn round the soma in distances of 50 μm. **D_{1-3}:** Axon collateral with multiple varicosities passes a spiny basal dendrite. A varicosity of the axon (open arrow) is located between two dendritic spines (filled arrows) suggesting an autaptic synaptic contact. For clarification the dendrite (D_2) and the axon (D_3) are illustrated separately. **E:** A main axon descending to the alveus closely passes a basal dendrite of the same cell also suggesting an autaptic site. Note that the axon is free of varicosities (see text). Scale bars = 100 μm in B (applies to A,B); 5 μm in D_3 (applies to D_{1-3}); 10 μm in E.

we did not find morphological differences of the dendritic system between regular- and burst-spiking pyramidal cells in the subiculum. In pilocarpine-treated rats (n = 10 cells) the morphology of both cell types did not show differences based on observational analysis. Due to the low fraction (30%) of burst-spiking cells in pilocarpine-treated rats, we pooled both cell types for statistical analysis. Our data indicate a seizure-induced layer-specific alteration of the proximal segment of the apical dendrites, which was evident by loss of spines and reduced branching. Dendritic spines are known to be modifiable cellular structures. As decreases in neuronal activity or the elimination of afferent pathways are generally thought to lead to a reduction in the number of postsynaptic spines (Parnavelas et al., 1974; Matthews et al., 1976; Calverley and Jones, 1990), this result suggests a partial deafferentiation due to a loss of CA1 cells and reduced axonal input. Aside from this, spine loss may also occur as a consequence of an enhanced neuronal activity and the excessive activation of postsynaptic glutamate receptors, as occurs during seizures. In particular, activation of NMDA

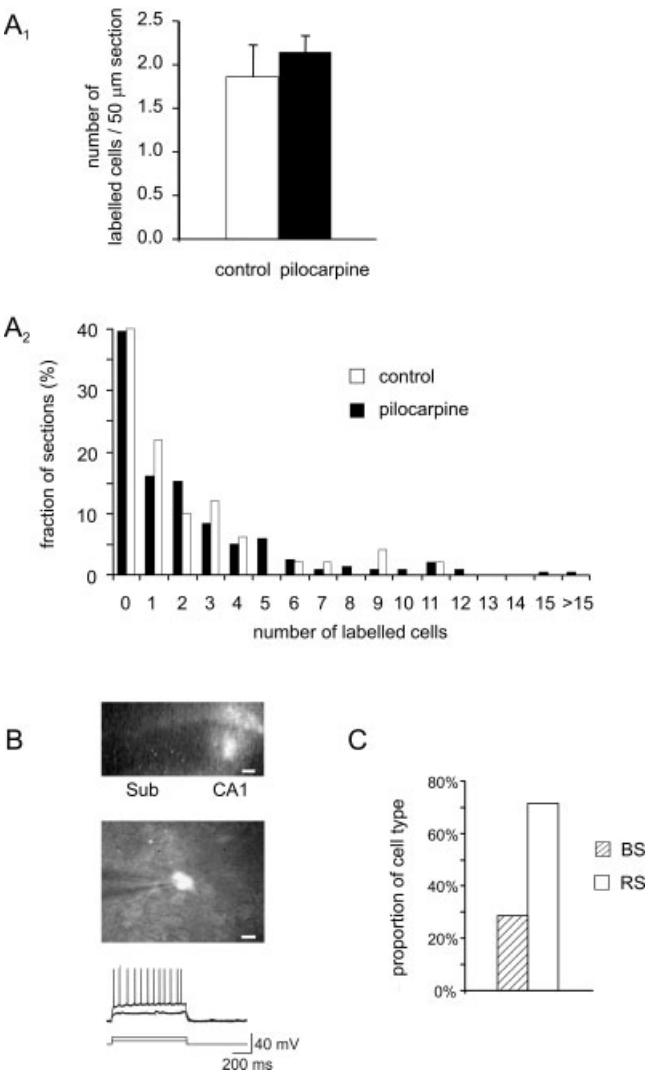

Fig. 8. Retrograde staining of subicular pyramidal cells by extracellular application of a fluorescence tracer in CA1. **A_1:** The average number of retrograde labeled subicular neurons per section (thickness 50 µm) was not different in control and pilocarpine-treated rats. **A_2:** Fraction of slices containing the same number of retrogradely stained neurons. No difference was found between control and pilocarpine-treated rats. **B:** Top: Slice stained with fluorescein in CA1. Middle: Same slice at higher magnification showing a patch-clamp electrode during recording of a retrogradely stained fluorescent subicular pyramidal cell. Bottom: Response of the same cell to a depolarizing current injection. The neuron was classified as a regular-spiking cell. **C:** Proportion of retrogradely labeled burst- and regular-spiking neurons in pilocarpine-treated rats. Scale bars = 200 µm in B, top; 20 µm in B, middle.

receptors and its associated Ca^{2+} influx may activate postsynaptic mechanisms that finally lead to the retraction of dendritic spines (Mattson et al., 1988; Siman et al., 1989; Halpain and Greengard, 1990). This result is reminiscent of studies in the kainate-model of epilepsy, where massive death of CA3 pyramidal cells is also followed by a rapid decrease in the number of spines in stratum radiatum of CA1 (Nadler et al., 1980; Phelps et al., 1991). However, in CA1 the number of synapses slowly recovers (Nadler et al., 1980), suggesting that a reactive synaptogenesis has taken place. In CA1 these newly formed synapses most likely originate from the formation of new recurrent associational fibers (Esclapez et al., 1999).

As the spine loss in pilocarpine-treated rats reduces the membrane surface, it might be associated with an increase of the cell's input resistance. However, we observed a reduction of the input resistance in subicular pyramidal cells from pilocarpine-treated rats, which suggests seizure-related conductance changes because it cannot be explained by the altered morphology. A reduction of the input resistance of subicular pyramidal cells of pilocarpine-treated rats was also described by Wellmer et al. (2002).

Axonal system

Extensive physiological data suggest that brain regions in which neurons are interconnected by a dense network of excitatory recurrent connections are particularly prone to seizures (Heinemann, 1987). Reconstructed axons of subicular pyramidal cells of control and pilocarpine-treated animals branched extensively throughout stratum pyramidale and the proximal part of the dendritic layer. The axons were lined with varicosities that are generally associated with synaptic contacts (Sik, 1993; Deuchars and Thomson, 1996; Vida et al., 1998). Therefore, it is likely that subicular pyramidal cells form synaptic contacts to adjacent neurons by recurrent collaterals. Frequently, axon collaterals crossed dendrites of the same cell at a distance of <1 µm, making it likely that subicular pyramidal cells form autaptic contacts with their own dendrites. This result may provide the morphological substrate for a high intrinsic connectivity and reciprocal interactions between subicular pyramidal cells. Reciprocal activity and the associated epiletogenic propensity of the subiculum was proposed by other electrophysiological studies (Behr and Heinemann, 1996; Harris and Stewart, 2001a,b).

Using both intracellular biocytin-staining and extracellular retrograde staining of subicular pyramidal cells, our data support the existence of an axonal projection from the subiculum back to stratum radiatum of CA1 (Berger et al., 1980; Köhler, 1985; Lehmann et al., 2001; Commins et al., 2001; Harris and Steward, 2001a,b; Harris et al., 2001). In pilocarpine-treated rats after SE and partial deafferentiation of CA1 from CA3, subicular pyramidal cells may sprout to vacated synaptic sites in CA1, as recently proposed (Lehmann et al., 2001). However, we have no evidence for a strengthened subicular-CA1 projection by aberrant sprouting of subicular fibers. Hence, the subiculum-CA1 projection seems to be physiological rather than a result of recurrent seizures.

In summary, most of the subicular network properties of pilocarpine-treated rats demonstrated in the present study do not seem to account for the enhanced excitability. The loss of subicular cells in pilocarpine-treated rats inherently implies an alteration of the cellular network. However, the reduced fraction of burst-spiking cells, spine-loss, and lack of axonal sprouting point rather to a decreased excitability of subicular pyramidal cells in epileptic rats. Polysynaptic afterdischarges in subicular pyramidal cells might be caused by an enhanced recurrent excitation via the reciprocal subiculum-EC-subiculum loop. In support of this hypothesis, the EC in patients suffering from TLE and several in vivo and in vitro models of TLE shows an increased susceptibility to seizures and

epileptiform discharges, respectively (Dasheiff and McNamara, 1982; Collins et al., 1983; Rutecki et al., 1989; Spencer and Spencer, 1994). However, due to the spare connectivity in brain slices between CA1-EC and EC-subiculum, this possibility is rather circumstantial in the present study.

In vitro studies of TLE (Behr and Heinemann, 1996; Menendez de la Prida and Gal, 2004) demonstrated that the isolated subiculum has the capacity to generate interictal and ictal-like activity. Like in hippocampal brain slices from TLE-patients (Cohen et al., 2002), hyperexcitabilty in slices obtained from pilocarpine-treated rats may be generated within the subiculum itself. In addition to network alterations, changes at the synaptic level, the site of neurotransmission, have been described extensively in human epileptic tissue and in various models of epilepsy. Tetanic stimulation as occurs during seizures was shown to result in stimulus-evoked polysynaptic discharges (Miles and Wong, 1987b; Charpier et al., 1995) by unmasking or enhancing weak synaptic connections. Particularly, seizure-induced modifications in GABAergic neurotransmission may cause attenuated or even depolarizing postsynaptic responses (Cohen et al., 2002). However, in pilocarpine-treated rats, but not in controls, the $GABA_A$ receptor antagonist bicuculline caused repetitive afterdischarges. Therefore, an altered activation of $GABA_A$ receptors is unlikely to be the only reason for the observed hyperexcitability. In different models of TLE and various regions of the hippocampus, seizures are known to increase the number of AMPA receptors (Abegg et al., 2003) and ease the activation of NMDA receptors (Ashwood and Wheal, 1987; Hirsch et al., 1996; Behr et al., 2001). Thus, strengthening of glutamatergic synapses seems to be an alternative explanation for repetitive afterdischarges in the subiculum of pilocarpine-treated rats.

Pathophysiological relevance

Brain structures exposed to persistent epileptiform activity can become epileptogenic, a process comparable to the kindling-phenomenon described by Goddard et al. (1967). This process of secondary epileptogenesis can be regarded as the development of a remote seizure focus in response to a primary seizure focus. In human TLE the CA3-CA1 regions are traditionally regarded as the primary hippocampal seizure foci. We believe that hippocampal seizures induce a secondary epileptogenesis downstream to CA1 in the subiculum. Our data indicate that, in contrast to CA1, neither an increase of burst-spiking cells nor axonal sprouting are mandatory for the enhanced excitability.

ACKNOWLEDGMENT

We thank S. Walden for excellent technical assistance.

LITERATURE CITED

Abegg MH, Savic N, Ehrengruber MU, McKinney RA, Gahwiler BH. 2004. Epileptiform activity in rat hippocampus strengthens excitatory synapses. J Physiol 554:439–448.

Amaral DG, Dolorfo C, Alvarez-Royo P. 1991. Organization of CA1 projections to the subiculum: a PHA-L analysis in the rat. Hippocampus 1:415–435.

Ashwood TJ, Wheal HV. 1987. The expression of N-methyl-D-aspartate-receptor-mediated component during epileptiform synaptic activity in hippocampus. Br J Pharmacol 91:815–822.

Behr J, Heinemann U. 1996. Low Mg2+ induced epileptiform activity in the subiculum before and after disconnection from rat hippocampal and entorhinal cortex slices. Neurosci Lett 205:25–28.

Behr J, Empson RM, Schmitz D, Gloveli T, Heinemann U. 1996. Electrophysiological properties of rat subicular neurons in vitro. Neurosci Lett 220:41–44.

Behr J, Gloveli T, Heinemann U. 1998. The perforant path projection from the medial entorhinal cortex layer III to the subiculum in the rat combined hippocampal-entorhinal cortex slice. Eur J Neurosci 10: 1011–1018.

Behr J, Heinemann U, Mody I. 2001. Kindling induces transient NMDA receptor-mediated facilitation of high-frequency input in the rat dentate gyrus. J Neurophysiol 85:2195–2202.

Berger TW, Swanson GW, Milner TA, Lynch GS, Thompson RF. 1980. Reciprocal anatomical connections between hippocampus and subiculum in the rabbit: evidence for subicular innervation of regio superior. Brain Res 183:265–276.

Boulton CL, von Haebler D, Heinemann U. 1992. Tracing of axonal connections by rhodamin-dextran-amine in the rat hippocampal-entorhinal cortex slice preparation. Hippocampus 2:99–106.

Calverley RK, Jones DG. 1990. Contributions of dendritic spines and perforated synapses to synaptic plasticity. Brain Res Rev 15:215–249.

Charpier S, Behrends JC, Triller A, Faber DS, Korn H. 1995. "Latent" inhibitory connections become functional during activity-dependent plasticity. Proc Natl Acad Sci U S A 92:117–120.

Cohen I, Navarro V, Clemenceau S, Baulac M, Miles R. 2002. On the origin of interictal activity in human temporal lobe epilepsy in vitro. Science 298:1418–1421.

Cohen I, Navarro V, Huberfeld G, Clemenceau S, Baulac M, Miles R. 2003. Response to Comment on "On the origin of interictal activity in human temporal lobe epilepsy in vitro." Science 301:463.

Collins RC, Tearse RG, Lothman EW. 1983. Functional anatomy of limbic seizures: focal discharges from medial entorhinal cortex in rat. Brain Res 280:25–40.

Commins S, Aggleton JP, O'Mara SM. 2002. Physiological evidence for a possible projection from dorsal subiculum to hippocampal area CA1. Exp Brain Res 146:155–160.

Crepel V, Khazipov R, Ben-Ari Y. 1997. Blocking GABA(A) inhibition reveals AMPA- and NMDA-receptor-mediated polysynaptic responses in the CA1 region of the rat hippocampus. J Neurophysiol 77:2071–2082.

Dasheiff RM, McNamara JO. 1982. Electrolytic entorhinal lesions cause seizures. Brain Res 231:444–450.

Deuchars J, Thomson AM. 1996. CA1 pyramid-pyramid connections in rat hippocampus in vitro: dual intracellular recordings with biocytin filling. Neuroscience 74:1009–1018.

Drakew A, Muller M, Gahwiler BH, Thompson SM, Frotscher M. 1996. Spine loss in experimental epilepsy: quantitative light and electron microscopic analysis of intracellularly stained CA3 pyramidal cells in hippocampal slice cultures. Neuroscience 70:31–45.

Du F, Eid T, Lothman EW, Köhler C, Schwarcz R. 1995. Preferential neuronal loss in layer III of the medial entorhinal cortex in rat models of temporal lobe epilepsy. J Neurosci 15:6301–6313.

Esclapez M, Hirsch JC, Ben-Ari Y, Bernard C. 1999. Newly formed excitatory pathways provide a substrate for hyperexcitability in experimental temporal lobe epilepsy. J Comp Neurol 408:449–460.

Finch DM, Babb TL. 1981. Demonstration of caudally directed hippocampal efferents in the rat by intracellular injection of horseradish peroxidase. Brain Res 214:405–410.

Finch DM, Nowlin NL, Babb TL. 1983. Demonstration of axonal projections of neurons in the rat hippocampus and subiculum by intracellular injection of HRP. Brain Res 271:201–216.

Fisher PD, Sperber EF, Moshe SL. 1998. Hippocampal sclerosis revisited. Brain Dev 20:563.

Gloveli T, Egorov AV, Schmitz D, Heinemann U, Muller W. 1999. Carbachol-induced changes in excitability and $[Ca^{2+}]_i$ signalling in projection cells of medial entorhinal cortex layers II and III. Eur J Neurosci 11:3626–3636.

Glover JC, Petursdottir G, Jansen JKS. 1986. Fluorescent dextran-amines used as axonal tracers in the nervous system of the chicken embryo. J Neurosci Methods 18:243–254.

Goddard GV. 1967. Development of epileptic seizures through brain stimulation at low intensity. Nature 214:1020–1021.

Greene JR. 1996. The subiculum: a potential site of action for novel antipsychotic drugs? Mol Psychiatry 1:380–387.

Halpain S, Greengard P. 1990. Activation of NMDA receptors induces

rapid dephosphorylation of the cytoskeletal protein MAP2. Neuron 5:237–246.

Harris E, Stewart M. 2001a. Intrinsic connectivity of the rat subiculum. II. Properties of synchronous spontaneous activity and a demonstration of multiple generator regions. J Comp Neurol 435:506–518.

Harris E, Stewart M. 2001b. Propagation of synchronous epileptiform events from subiculum backward into area CA1 of rat brain slices. Brain Res 895:41–49.

Harris E, Witter MP, Weinstein G, Stewart M. 2001. Intrinsic connectivity of the rat subiculum. I. Dendritic morphology and patterns of axonal arborization by pyramidal neurons. J Comp Neurol 435:490–505.

Heinemann U. 1987. Basic mechanisms of the epilepsies. In: Halliday AM; Butler SR, Paul R, editors. A textbook of clinical neurophysiology. New York: John Wiley & Sons. p 497–534.

Hirsch JC, Quesada O, Esclapez M, Gozlan H, Ben-Ari Y, Bernard CL. 1996. Enhanced $NMDA_R$-dependent epileptiform activity is controlled by oxidizing agents in a chronic model of temporal lobe epilepsy. J Neurophysiol 76:4185–4189.

Isokawa M, Levesque MF. 1991. Increased NMDA responses and dendritic degeneration in human epileptic hippocampal neurons in slices. Neurosci Lett 132:212–216.

Jensen MS, Yaari Y. 1997. Role of intrinsic burst firing, potassium accumulation, and electrical coupling in the elevated potassium model of hippocampal epilepsy. J Neurophysiol 77:1224–1233.

Jung HY, Staff NP, Spruston N. 2001. Action potential bursting in subicular pyramidal neurons is driven by a calcium tail current. J Neurosci 21:3312–3321.

Köhler C. 1985. Intrinsic projections of the retrohippocampal region in the rat brain. I. The subicular complex. J Comp Neurol 236:504–522.

Lehmann T-N, Gabriel S, Eilers A, Njunting M, Kovacs R, Schulze K, Lanksch WR, Heinemann U. 2001. Fluorescent tracer in pilocarpine-treated rats shows widespread aberrant hippocampal neuronal connectivity. Eur J Neurosci 14:83–95.

Mason A. 1993. Electrophysiology and burst-firing of rat subicular pyramidal neurons in vitro: A comparison with area CA1. Brain Res 600: 174–178.

Mathern GW, Babb TL, Armstrong DL. 1997. Hippocampal sclerosis. In: Engel J Jr, Pedley TA, editors. Epilepsy: a comprehensive textbook. Philadelphia: Lippincott-Raven. p 133–155.

Matthews DA, Cotman C, Lynch G. 1976. An electron microscopic study of lesion-induced synaptogenesis in the dentate gyrus of the adult rat. I. Magnitude and time course of degeneration. Brain Res 115:1–21.

Mattia D, Hwa GG, Avoli M. 1993. Membrane properties of rat subicular neurons in vitro. J Neurophysiol 70:1244–1248.

Mattia D, Kawasaki H, Avoli M. 1997. Repetitive firing and oscillatory activity of pyramidal-like bursting neurons in the rat subiculum. Exp Brain Res 114:507–517.

Mattson MP, Dou P, Kater SB. 1988. Outgrowth-regulating actions of glutamate in isolated hippocampal pyramidal neurons. J Neurosci 8:2087–2100.

Menendez de la Prida L. 2003. Control of bursting by local inhibition in the rat subiculum in vitro. J Physiol 549:219–230.

Menendez de la Prida L, Gal B. 2004. Synaptic contributions to focal and widespread spatiotemporal dynamics in the isolated rat subiculum in vitro. J Neurosci 24:5525–5536.

Menendez de la Prida L, Suarez F, Pozo MA. 2003. Electrophysiological and morphological diversity of neurons from the rat subicular complex in vitro. Hippocampus 13:728–744.

Miles M, Wong RK. 1987a. Inhibitory control of local excitatory circuits in the guinea-pig hippocampus. J Physiol 388:611–629.

Miles R, Wong RK. 1987b. Latent synaptic pathways revealed after tetanic stimulation in the hippocampus. Nature 329:724–726.

Nadler JV, Perry BW, Gentry C, Cotman CW. 1980. Loss and reacquisition of hippocampal synapses after selective destruction of CA3-CA4 afferents with kainic acid. Brain Res 191:387–403.

O'Mara SM, Commins S, Anderson M, Gigg J. 2001. The subiculum: a review of form, physiology and function. Prog Neurobiol 64:129–155.

Parnavelas JG, Lynch G, Brecha N, Cotman CW, Globus A. 1974. Spine loss and regrowth in hippocampus following deafferentiation. Nature 248:71–73.

Perez Y, Morin F, Beaulieu C, Lacaille JC. 1996. Axonal sprouting of CA1 pyramidal cells in hyperexcitable hippocampal slices of kainate-treated rats. Eur J Neurosci 8:736–748.

Phelps S, Mitchell J, Wheal HV. 1991. Changes to synaptic ultrastructure in field CA1 of the rat hippocampus following intracerebroventricular injection of kainic acid. Neuroscience 40:687–699.

Rutecki PA, Grossman RG, Armstrong D, Irish-Loewen S. 1989. Electrophysiological connections between the hippocampus and entorhinal cortex in patients with complex partial seizures. J Neurosurg 70:667–675.

Sanabria ER, Su H, Yaari Y. 2001. Initiation of network bursts by Ca2+-dependent intrinsic bursting in the rat pilocarpine model of temporal lobe epilepsy. J Physiol 532:205–216.

Scheibel ME, Crandall PH, Scheibel AB. 1974. The hippocampal-dentate complex in temporal lobe epilepsy. A Golgi study. Epilepsia 15:55–80.

Sik A, Tamamaki N, Freund TF. 1993. Complete axon arborization of a single CA3 pyramidal cell in the rat hippocampus, and its relationship with postsynaptic parvalbumin-containing interneurons. Eur J Neurosci 5:1719–1728.

Siman R, Noszek JC, Kegerise C. 1989. Calpain I activation is specifically related to excitatory amino acid induction of hippocampal damage. J Neurosci 9:1579–1590.

Smith BN, Dudek FE. 2001. Short- and long-term changes in CA1 network excitability after kainate treatment in rats. J Neurophysiol 85:1–9.

Spencer SS, Spencer DD. 1994. Entorhinal-hippocampal interactions in medial temporal lobe epilepsy. Epilepsia 35:721–727.

Staff NP, Jung HY, Thiagarajan T, Yao M, Spruston N. 2000. Resting and active properties of pyramidal neurons in subiculum and CA1 of rat hippocampus. J Neurophysiol 84:2398–2408.

Steward O, Scoville SA. 1976. Cells of origin of entorhinal cortical afferents to the hippocampus and fascia dentata of the rat. J Comp Neurol 169:347–370.

Stewart M. 1997. Antidromic and orthodromic responses by subicular neurons in rat brain slices. Brain Res 769:71–85.

Su H, Sochivko D, Becker A, Chen J, Jiang Y, Yaari Y, Beck H. 2002. Upregulation of a T-type Ca2+ channel causes a long-lasting modification of neuronal firing mode after status epilepticus. J Neurosci 22:3645–3655.

Tamamaki N, Nojyo Y. 1990. Disposition of the slab-like modules formed by axon branches originating from single CA1 pyramidal neurons in the rat hippocampus. J Comp Neurol 291:509–519.

Taube JS. 1993. Electrophysiological properties of neurons in the rat subiculum in vitro. Exp Brain Res 96:304–318.

Turski L, Ikonomidou C, Turski WA, Bortolotto ZA, Cavalheiro EA. 1989. Review: cholinergic mechanisms and epileptogenesis. The seizures induced by pilocarpine: a novel experimental model of intractable epilepsy. Synapse 3:154–171.

van Groen T, Miettinen P, Kadish I. 2003. The entorhinal cortex of the mouse: organization of the projection to the hippocampal formation. Neuroscience 119:1185–1197.

Vida I, Halasy K, Szinyei C, Somogyi P, Buhl EH. 1998. Unitary IPSPs evoked by interneurons at the stratum radiatum-stratum lacunosum-moleculare border in the CA1 area of the rat hippocampus in vitro. J Physiol 506:755–773.

Walker MC, White HS, Sander JW. 2002. Disease modification in partial epilepsy. Brain 125:1937–1950.

Wellmer J, Su H, Beck H, Yaari Y. 2002. Long-lasting modification of intrinsic discharge properties in subicular neurons following status epilepticus. Eur J Neurosci 16:259–266.

Witter MP. 1993. Organization of the entorhinal-hippocampal system: a review of current anatomical data. Hippocampus 3 Spec No 33–44.

Witter MP, Amaral DG. 1991. Entorhinal cortex of the monkey. V. Projections to the dentate gyrus, hippocampus, and subicular complex. J Comp Neurol 307:437–459.

Witter MP, Groenewegen HJ. 1990. The subiculum: cytoarchitectonically a simple structure, but hodologically complex. Prog Brain Res 83:47–58.

Witter MP, Ostendorf RH, Groenewegen HJ. 1990. Heterogeneity in the dorsal subiculum of the rat. Distinct neuronal zones project to different cortical and subcortical targets. Eur J Neurosci 2:718–725.

Wozny C, Kivi A, Lehmann TN, Dehnicke C, Heinemann U, Behr J. 2003. Comment on "On the origin of interictal activity in human temporal lobe epilepsy in vitro." Science 301:463.

Yaari Y, Beck H. 2002. "Epileptic neurons" in temporal lobe epilepsy. Brain Pathol 12:234–239.